반도체 칩의 범프 불량 검사를 위한 정확한 경계 검출 알고리즘

김 은 석*

Accurate Boundary detection Algorithm for The Faulty Inspection of Bump On Chip

EUNSEOK KIM*

요 약

제안된 방법은 다른 이미지 서브트랙션 방법에 대하여 커다란 성능향상을 보임을 일련의 실험들을 통하여 보여준다. 일반적으로 수 마이크로 단위로 계측되는 반도체의 검사 정밀도를 높이기 위해서는 라인스캔 카메라가 이용된다. 그러나 불량 검사는 스캔속도와 조명조건에 매우 민감하기 때문에 정확한 경계 검출 알고리즘이 필요하다.

본 논문에서는 반도체 칩의 범프 불량 검출의 정확성을 높이기 위해서 서브픽셀을 적용한 경계 검출을 제안하였다. 범프 에지는 범프 중심점에서 네 방향으로 1차 도함수에 의해서 검출되고 서브픽셀 방법으로 정확한 에지 위치를 찾는다. 그리고 범프 돌기, 범프 브리지, 범프 변색에 의해 범프 크기가 변할 수 있기 때문에 에러를 최소화 하기 위해서 최소자승법을 이용하여 정확한 범프 경계를 구한다.

실험 결과 제안된 방법은 기존의 다른 경계 검출 알고리즘에 비하여 커다란 성능향상을 보였다.

ABSTRACT

Generally, a semiconductor chip measured with a few micro units is captured by line scan camera for higher inspection accuracy. However, the faulty inspection requires an exact boundary detection algorithm because it is very sensitive to scan speed and lighting conditions.

In this paper we propose boundary detection with subpixel edge detection in order to increase the accuracy of bump faulty detection on chips. The bump edge is detected by first derivative to four directions from bump center point and the exact edge positions are searched by the subpixel method. Also, the exact bump boundary to calculate the actual bump size is computed by LSM(Least Squares Method) to minimize errors since the bump size is varied such as bump protrusion, bump bridge, and bump discoloration.

Experimental results exhibit that the proposed algorithm shows large improvement comparable to the other conventional boundary detection algorithms.

키워드

line scan camera, boundary detection, subpixel, first derivative

Ⅰ. Introduction

Recently, the integration degree of semiconductor chips has been increased according to product miniaturization and technique diversification. The integrated trend of semiconductor products has many advantages to increase

* 아주대학교 산업공학과

접수일자 : 2006. 9. 26

arrangement efficiency since it is gradually developed in the form of low profile and small form factor, multi-function, multi-pin process, etc. The Chip on Glass (COG) is a method to adhere the Bare Die(IC) to the glass panel. The COG process is as follows: After a wafer comes in, the tape mount to attach the blackout tape on the back of the wafer is accomplished and then cutting process to separate the wafer die individually is performed. The defective items of the COG are classified into the bump defect and the inner chip defect, where the bump means an protruded electrode that connects an electrode on chip to an electrode on a circuit board. And the detailed defects of bump are categorized into a wrong bump size, no bump, a bump discoloration, a bump protrusion, and a bump bridge. The wrong bump size and no bump occurs when the calculated bump sizes are smaller or larger than designed bump size. If these defects arise, the bumps are not able to be connected to the electrode on circuit board. The bump discoloration is a factor to influence the electric characteristics and reliability. Also, the bump protrusion is a factor to affect into neighbor bumps, and the bump bridge is a case to make the equal electrode since two neighbor bumps are connected each other. Up until now, the defective inspection of the COG has made an effect on the quality reliability due to the naked eye measurement, but the defective inspection by the machine vision has an effect on improving the quality and the productivity. The template matching, the statistical[1,2], the syntactic[3], and the neural network method[4,5,7] are generally applied to inspect precision examination like the semiconductors in machine vision.

The COG image is captured by line scan camera for precise inspection. The distortion occurs on the captured image due to sensitiveness of scan speed, and the captured images show different brightness distribution under different lighting conditions. These various problems have given rise to difficulties in inspection automation.

In this paper, we present the robustness boundary detection algorithm using subpixel to enhance the accuracy of COG bump defective detection in variable environment conditions. The bump protrusion, the bump bridge, and a particle around the bump are of great effects on the exact bump boundary detection. To recognize accurate boundary, therefore, we compute an approximate bump edge using a partial differentiation in the four directions from the bump center coordinates, followed by computation of the accurate bump edges using the subpixel.

Ⅱ. A defective detection initialization

Initializing step of the defective detection is as follows: Firstly, the chip image which contains no defect item but has an identical pattern is captured by line scan camera since the pattern is varied according to chip kinds. Furthermore, the conditions which can change the image size and brightness due to the scan speed and lighting condition despite the identical pattern must be considered. Secondly, we select the four template images at the four corners on COG image. Finally, we search the bump position and boundary.

While the bump boundary is detected by the 8-direction chain code method, the center point of the bump is searched by the pixel-values of the bump round as shown in eq. 1. The center coordinates of two templates are applied to calculate chip angle on the base line as shown in Fig. 1. Also, the center coordinates of two templates are appropriated to calculate the relative coordinates of bumps.

The bump size and brightness are calculated using average of all bumps to prevent distortions by scan speed and lighting conditions.

$$c_x = \frac{1}{n}\sum_{i=1}^{n} x_i,\ c_y = \frac{1}{n}\sum_{j=1}^{n} y_i \tag{1}$$

Where,

c_x, c_y : the center point of a bump

x_i, y_i: x, y coordinates of an edge

n : boundary number of a bump

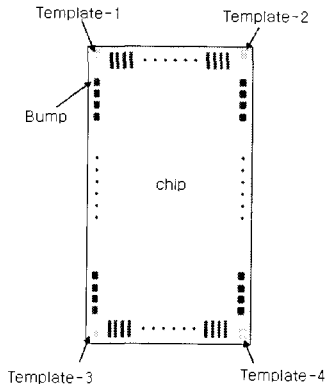

Fig. 1 The four templates and bumps on chip.

Ⅲ. A defective detection algorithm

Since pattern, size, and position are varied according to COG kinds after the basic parameters such as the relative center coordinates of bumps, the bump size, and the bump discoloration are set up according to patterns, the defect detection algorithm on the input real image is applied. The defective detection procedure is as follows: Firstly, we reckon the center coordinates of templates on the input image using a statistical pattern cognition method. Secondly, we calculate the approximate relative center coordinates of bumps from a template. Thirdly, we compute the bump protrusion, the bump bridge, and the bump discoloration after detecting the bump boundary on the input image.

3.1 The template matching

The center coordinates of a template are calculated with the statistical pattern cognition which is able to verify the matching degree between the template on the input image and the template on the reference image. The eq. 2 is an equation to estimate a correlation coefficient between the template on the input image and the template on the reference image. To recognize rotation angle between template 1 and template 2, the template matching[1,2] between reference and input image on the basis of the template center coordinates is adopted.

Also, the approximate center coordinates of bumps which require the boundary detection of bumps are computed by the rotation and shift transformation. Though the center coordinates of bumps have the coordinate error because of the matching error, the exact center coordinates of bumps can be reckoned using the boundary detection algorithm.

$$r = \frac{\sum_{i=0}^{M-1}\sum_{j=0}^{N-1} a(i,j)b(i,\ j)}{\sqrt{\sum_{i=0}^{M-1}\sum_{j=0}^{N-1} a(i,j)^2 \times \sum_{i=0}^{M-1}\sum_{j=0}^{N-1} b(i,j)^2}} \qquad (2)$$

Where,

r = Correlation coefficient

$g(i,\ j)$: the approximate template area of input image

$t(i,\ j)$: the template area of reference image

$\overline{m}$: average of $g(i,\ j)$

$\bar{t}$: average of $t(i,\ j)$

$a(i,\ j) = g(i,\ j) - \overline{m}$

$b(i,\ j) = t(i,\ j) - \bar{t}$

M: horizontal size of template image

N: vertical size of template image

3.2 The Boundary detection algorithm

The detection algorithm recognizes boundary which includes bump protrusion and bridge. To detect bump boundary, the center coordinates of template on the input image are calculated using template matching between reference and input image. The approximate center coordinates of bumps are found based the template center coordinate on the input image and the relative bumps' coordinates set on the reference image. The bump boundary is detected in four directions based on the bump center coordinates.

The Fig. 2 shows the bump boundary detection on y axis direction. To detect exact boundary on two side boundaries(W, E) in the Fig. 2, the partial differential based on y-axis direction is used on each side. If the partial differential value is greater than the predetermined threshold, then the point is recognized with exact boundary point. However, in case of bump bridge, the partial

differential value which is greater than the threshold does not exist since the both of the side bumps are connected. In this case the maximum x coordinate in detection direction is stored with boundary x coordinate.

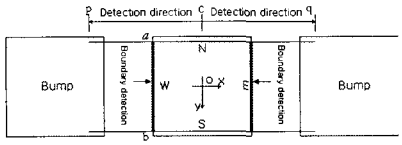

Fig. 2 Boundary detection to $+x$ and $-x$ direction from bump center point.

The Fig. 3 shows the bump boundary detection on x axis direction. To detect exact boundary on two side boundaries(N, S), the partial differential based on x-axis direction is used on each side. The boundary recognizing precess of bump is identical with y-axis searching method.

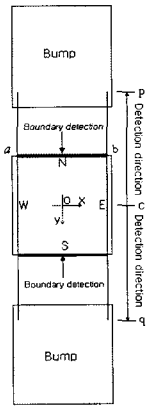

Fig. 3 Boundary detection to $+y$ and $-y$ direction from bump center point.

3.3 The exact edge measurement using the subpixel

Since bump faulty items are determined with a few micro unit and the miniature boundary detection algorithm is required, the edge coordinates are revised using the subpixel method[6]. Typical edge profiles observed in real images reveal the near step-edge as shown in Fig. 4(a). The exact edge of the step-edge can be the extreme point of the first derivative. To estimate the value of the extreme accurately, we approximate the first derivative's distribution by a curve of the second-order polynomial.

Assume that pixel j_0 is the nearest to an actual edge position and the values of the gradient magnitudes at pixel j_0-1, j_0, and j_0+1 are g_{j_0-1}, g_{j_0}, g_{j_0+1}, respectively. A second-order polynomial in eq. 3 is used to approximate the gradient magnitude near the edge. In case the brightness decreases monotonously as A in the Fig. 4, $x_{\min}$ is found using Eq 4. In case of opposite, $x_{\max}$ is calculated using Eq. 5. And x_{min} and $x_{\max}$ means the exact boundary position of a bump.

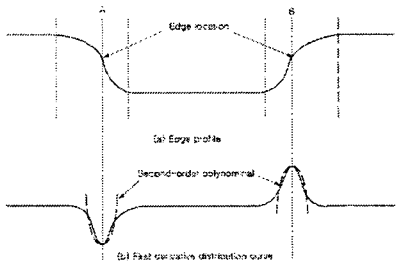

Fig. 4 Edge profile and first derivative distribution curve.

$$y = a(x-j_0)^2 + b(x-j_0) + c \tag{3}$$

Where,

$$a = \frac{g_{j_0-1} - 2g_{j_0} + g_{j_0+1}}{2}$$

$$b = \frac{g_{j_0+1} + g_{j_0-1}}{2}$$

$$c = g_{j_0}$$

$$x_{\max} = j_0 - \frac{b}{2a} \tag{4}$$

$$x_{\min} = j_0 + \frac{b}{2a} \tag{5}$$

3.4 The center coordinates and detective detection of bumps

The real center coordinates of bumps can be reckoned with the four direction boundaries and the least square even though the bump boundaries include the noise. The measurement procedure is as follows: To compute the

regression line in each direction after boundary coordinates in each direction are substituted into Eq (7) and (8), regression line as Eq (6) is calculated. The vertex and center point of a bump using intersection points of four regression lines are counted. Although somewhat wrong boundary is detected, the least square can obtain real proximity boundary line.

$$\hat{y}=\hat{\beta}_0+\hat{\beta}_1 x+\varepsilon_i \tag{6}$$

$$\hat{\beta}_1=\frac{\sum(x_i-\bar{x})(y_i-\bar{y})}{\sum(x_i-\bar{x})^2} \tag{7}$$

$$\hat{\beta}_0=\bar{y}-\hat{\beta}_1\bar{x} \tag{8}$$

Where,

$\varepsilon_i \sim N(0,\sigma^2)$: an error term

$\hat{\beta}_0$: y intercept of an unknown population number

$\hat{\beta}_1$: gradient of an unknown population number

$i=1,2...,n$

To detect bump protrusion and bridge the four direction boundaries of a bump and its regression lines are applied. The Fig. 5 displays extracted bump boundaries by the four bump boundary regression lines and boundary detection algorithm. The bump protrusion in the E and W direction can be determined using the difference between x coordinates between regression line and bump boundary. Furthermore, the bump protrusion in the S, N direction can be judged using the difference between y coordinates between regression line and bump boundary.

If the difference value is greater than predetermined value between each bump, the bump bridge is concluded. In case of smaller than predetermined value, the bump protrusion is decided.

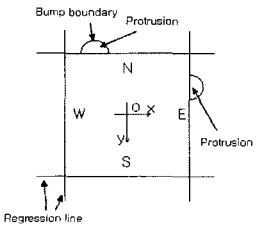

Fig. 5 The bump protrusion and regression line.

The bump discoloration occurs in case of the oxidized reaction and scratch of bump. To detect the bump discoloration, we apply the weighted brightness for all pixels of a bump between the reference and the input image. If the brightness difference for all pixels is greater than predetermined threshold, this bump is determined as discolored bump.

Ⅳ. The experimental results

The vision system used in this research to inspect the 16,670 x 2,430 COG dimension consists with 2K line scan camera and Matrox image board, programming language is Visual C++ under window 2000.

The defective detection precess of bumps on the input image is as follows: After the reference image which has no defect is captured, we reckon the relative coordinate from the center coordinates of templates to the each bumps as shown Fig. 6 and set up the predetermined parameter according to chip kinds as shown table 1. The angle between the two templates and the center coordinates of templates are calculated by template matching between reference and input image. The approximated center coordinates of bumps are computed by the coordinates transformation from the center coordinates of templates.

Table 2 denotes the average recognition time and rate of templates about 50 input test images. In table 2, the recognition rate of four templates is more than 92 percent. Since the average difference between the approximated and real center coordinates of bumps is about ±4 pixel error, the errors are deliberated at searching parameter setting on the input image, as shown in table 3.

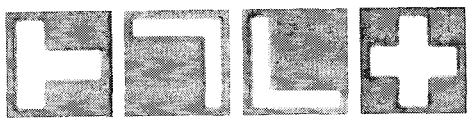

Fig. 6 Four template images.

Table. 1 The parameter value of reference image.

Parameter(reference image)	Value
Template1 and 2 angle	0.1°
Average bump size	95×20pixel
Average gray level of bump	36
Minimum pixel difference between interior and exterior of bump	56

Table.2 Average recognition rate and recognition time of templates. (Chips : 50)

	Template1	Template2	Template3	Template4
Average time(sec)	0.531	0.59	0.595	0.516
Average recognition rate	94.2%	92.8%	93%	93.6%

Table.3 The range of parameter value in input image.

Parameter(input image)	Range	
	Minimum	Maximum
Angle between template1 and template2	-1°	+1°
Gray level range of bump	30	42
Pixel position error of center point	-4	+4

The Fig. 7 and 8(a) show the bump protrusion and the bridge case. The applied results of proposal algorithm in this paper are displayed in the Fig. 7 and 8(b). The bump boundary by Laplacian is not practically detected, as shown in Fig. 7 and 8(c). The boundary detection result is better than Laplacian applying result. However, the bump protrusion is not mostly recognized, as demonstrated in Fig. 8(d). we calculate the weighted brightness for all pixels of a bump between the reference and the input image, as given in Fig. 9. The recognition rate of bump faulty items in table 4 represents 100 percent except the bump protrusion.

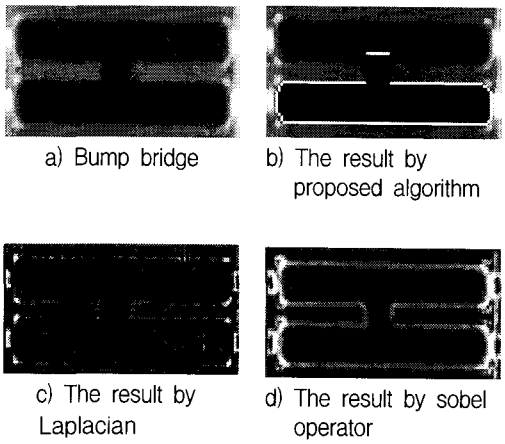

a) Bump bridge b) The result by proposed algorithm

c) The result by Laplacian d) The result by sobel operator

Fig. 7 The bump bridge.

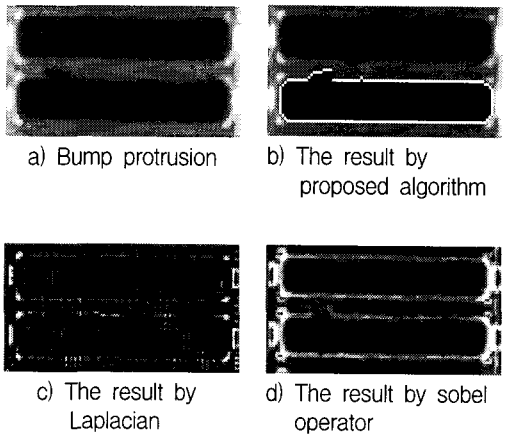

a) Bump protrusion b) The result by proposed algorithm

c) The result by Laplacian d) The result by sobel operator

Fig. 8 The bump protrusion.

Fig. 9 The bump fading.

Table. 4 A recognition rate and permissible range of bump faultiness

Bump faulty	Recognition rate	Tolerance limit
Bump size	100%	±4(pixels)
Bump discoloration	100%	±20(gray-level)
Bump protrusion	98%	±2(pixels)
Bump bridge	100%	

V. Conclusion

To make improvements in the inspection accuracy of COG the COG images is captured by line scan camera. Some distortions, however, occur on the captured image due to sensitiveness of scan speed and thereby the captured images are the different brightness distribution according to lighting conditions. In this paper, we proposed the robust bump defect inspection algorithm under variable environment conditions. To detect the bump defects the bump boundary was detected by partial differential to four directions based on bump center point and the exact boundary positions were searched by subpixel methods. And the regression line in each direction of bump was calculated with the least square.

In the experimental results using proposed method the defective recognition rate of bump is 100 percent except the bump protrusion even though the pattern, size, and position are varied according to COG kinds. Consequently, the field test results have greatly improved comparable to the naked eye measurement.

참고문헌

[1] Zheng, Z., Wang, H. and Teoh, K., "Analysis of gray level corner detection," Pattern Recognition Letters, Vol.20, pp. 149-162, 1999.

[2] A. Roddy and J. Stosz, "Fingerprint Features: Statistical Analysis and System Performance Estimates," Proc. of IEEE, Vol. 85, No.9, pp. 1390-1421, 1997.

[3] L. S. Oliveira, R. Sabourin, F. Bortolozzi, and C. Y. Suen, "Automatic recognition of handwritten numerical strings: A recognition and verification strategy," IEEE Trans. on PAMI, vol. 24, no. 11, pp. 1438-1454, 2002.

[4] Jie Yang, Hua Yu, "A Direct LDA Algorithm for High-Dimensional Data with Application to Face Recognition." Pattern Recognition 34(10), pp. 2067-2070, 2001.

[5] Jeong, S. W., Kim, S. H. and Cho, W. H., "Performance comparison of statistical and neural network classifiers in hand-written digits recognition," Proc. 6th IWFHR, Taejon, pp. 419-428, 1998.

[6] Ohtani K., Baba M., "A Fast Edge Location Measurement with Subpixel Accuracy Using a CCD Image," Proc. of IEEE, Vol. 3, No. 3, pp. 2087-2092, 2001.

[7] Chen-Hung Huang, Chi-Feng Wu, Chua-Chin Wan, "Image processing techniques for wafer cluster identification," IEEE Design & Test of computers, vol. 19, no. 2, pp. 44-48, 2002.

저자소개

김 은 석(Eun-Seok Kim)

2001 목포해양대학교, 해양정보통신학과 석사
2006 아주대학교, 산업공학과 박사
2004 - 2005 이알하우스 기술연구소
2005 - 현재 제노시스(주) 기술연구소
※관심분야 : 머신비전, 3D 측정, 패턴인식